Audio-frequency surface wave characteristics above porous and comb-like surfaces

Keith Attenborough[1]
The Open University
School of Engineering and Innovation, Walton Hall, Milton Keynes, MK7 6AA, UK

Shahram Taherzadeh[2]
The Open University
School of Engineering and Innovation, Walton Hall, Milton Keynes, MK7 6AA, UK

ABSTRACT

Near grazing incidence, the sound field due to point sources over porous or comb-like boundaries can include an airborne surface wave. Analytical expressions for the phase and group speeds of this surface wave are obtained using (i) a thin air layer approximation for the impedance of a comb-like surface, (ii) two approximate models for the acoustical properties of porous media and (iii) a model for a surface consisting of identical parallel slanted slits above a hard plane. Comparisons of model predictions indicate that the approximate model, derived initially to predict the acoustical properties of porous asphalt, is the least accurate. Predictions of surface wave attenuation and group velocity are compared with data obtained over arrays of parallel aluminium strips.

1. INTRODUCTION

Part of the solution for the sound field due to a point source in air over a porous or comb-like boundary has the form of an airborne surface wave which spreads cylindrically but attenuates both away from and along the surface [1]. Such waves have been observed over thin, low flow resistivity layers at ultrasonic frequencies [2], and at audio-frequencies [3, 4]. They have been observed over rough surfaces when the roughness height and spacing are small compared with the incident wavelength [5].

1.1. Approximate analytic expressions for phase and group speeds

Assuming Cartesian coordinates (x, y, z), the velocity potential of a wave travelling in the x-direction above a surface of admittance β parallel to the x-y plane is represented by

$$\phi(x, y, z, t) = F(x)e^{-i\omega t}e^{i\gamma x}e^{i\delta z} \tag{1}$$

where $F(x)$ accounts for geometrical spreading, ω is the angular frequency, γ and δ are the propagation constants in the horizontal and vertical directions respectively.

The vertical δ and horizontal γ wave numbers are given by [3]

[1] keith.attenborough@open.ac.uk
[2] Shahram.Taherzadeh@open.ac.uk

$$\delta = k_0\beta, \gamma = k_0\sqrt{1-\beta^2} \tag{2}$$

where, $k_0 = \omega/c_0$ is the propagation constant in air, ω is the angular frequency, c_0 is the free-space adiabatic sound speed, and ρ_0 is the air density.

One of the requirements for a surface wave to be created by point source excitation near an impedance plane is that the imaginary part of the surface impedance (X) is much larger than the real part (R) [1]. If $X \gg R$,

$$\mathrm{Im}(\gamma) \approx k_0(R/X^3), \mathrm{Im}(\delta) \approx k_0/X, \tag{3}$$

indicating that the attenuation along the surface is much smaller than the attenuation away from it.

The phase speed, c_p, of the surface wave above a hard-backed layer of thickness d and surface admittance $\beta(d)$ is given by

$$c_p = \frac{c_0}{\sqrt{1-\beta(d)^2}} \tag{4}$$

and the group speed c_g is given by

$$c_g = \frac{c_0\sqrt{1-\beta(d)^2}}{1-\beta(d)^2-\omega\beta(d)(d\beta(d)/d\omega)}. \tag{5}$$

For a hard-backed layer with characteristic admittance β and propagation constant k

$$\beta(d) = -i\beta\tan(kd) \tag{6a}$$

From (6a)

$$\frac{d\beta(d)}{d\omega} = -i\left\{\frac{d\beta}{d\omega}\tan(kd) + \beta d[1+(\tan(kd))^2]\frac{dk}{d\omega}\right\}. \tag{6b}$$

If a hard-backed thin air layer of thickness d is used to approximate the surface impedance of a comb-like boundary, then $\beta(d) = -i\rho_0 c_0\tan(k_0 d)$ and $d\beta(d)/d\omega = \frac{-id}{c_0}[1+(\tan(k_0 d))^2]$. For other models, analytical expressions for phase and group speeds of the surface wave are obtained by substituting expressions for characteristic admittance, surface admittance, propagation constant and appropriate derivatives in equations (4) and (5).

Approximate expressions for the characteristic impedance and propagation constant of a porous medium with flow resistivity R_s, porosity Ω, and tortuosity T, and intended to model the acoustical properties of porous asphalt [6] (henceforth called the Hamet model), may be written

$$Z_H = \left(\frac{\rho_0 c_0}{\Omega}\right)\sqrt{T}\left\{\gamma-(\gamma-1)\left(\frac{1}{F_0}\right)\right\}^{-1/2}F_\mu^{1/2}, k_H = k_0\sqrt{T}\left\{\gamma-(\gamma-1)\left(\frac{1}{F_0}\right)\right\}^{1/2}F_\mu^{1/2} \tag{7}$$

where $F_\mu = 1 + i\,\omega_\mu/\omega$, $F_0 = 1 + i\,\omega_0/\omega$, $\omega_\mu = (R_s/\rho_0)(\Omega/T)$, $\omega_0 = \omega_\mu(T/N_{PR})$ and N_{PR} is the Prandtl number.

The Hamet model results in the following expressions for the derivatives required for group speed calculations

$$\frac{d\beta_H}{d\omega} = \left(\frac{i\Omega^2 R_S}{2\omega^2\rho_0\sqrt{T}}\right)\frac{1}{\sqrt{1+\frac{i}{\omega}\left(\frac{\Omega R_S}{\rho_0 T}\right)}}\left\{\left(\frac{1}{T}\right)\frac{\sqrt{\gamma-(\gamma-1)\left(1+\frac{i\Omega R_S}{\omega\rho_0 N_{PR}}\right)^{-1}}}{1+\frac{i}{\omega}\left(\frac{\Omega R_S}{\rho_0 T}\right)} - \left(\frac{1}{\rho_0 N_{PR}}\right)\left[\frac{(\gamma-1)}{\sqrt{\gamma-(\gamma-1)\left(1+\frac{i\Omega R_S}{\omega\rho_0 N_{PR}}\right)^{-1}\left(1+\frac{i\Omega R_S}{\omega\rho_0 N_{PR}}\right)^2}}\right]\right\}, \tag{8a}$$

$$\frac{dk_H}{d\omega}=\frac{T}{c_0}\sqrt{\gamma-(\gamma-1)\left(1+\frac{i\Omega R_s}{\omega\rho_0 N_{PR}}\right)^{-1}}\sqrt{1+\frac{i}{\omega}\left(\frac{\Omega R_s}{\rho_0 T}\right)}\times$$
$$\left\{1-\frac{i\Omega R_s}{2\omega\rho_0 N_{PR}}\left[\frac{\left(\gamma-(\gamma-1)\left(1+\frac{i\Omega R_s}{\omega\rho_0 N_{PR}}\right)^{-1}\right)^{-1}}{\left(1+\frac{i\Omega R_s}{\omega\rho_0 N_{PR}}\right)^{-2}}-\left(1+\frac{i}{\omega}\left(\frac{\Omega R_s}{\rho_0 T}\right)\right)^{-1}\right]\right\}. \quad (8b)$$

According to the relaxation model due to Wilson [7], the characteristic impedance and propagation constant of a porous material may be written

$$Z_W=\frac{\sqrt{T}}{\Omega}\left[\left(1+\frac{\gamma-1}{\sqrt{1-i\omega\tau_e}}\right)\left(1-\frac{1}{\sqrt{1-i\omega\tau_v}}\right)\right]^{-1/2},$$
$$k_W=\frac{\omega\sqrt{T}}{c_0}\left[\left(1+\frac{\gamma-1}{\sqrt{1-i\omega\tau_e}}\right)\Big/\left(1-\frac{1}{\sqrt{1-i\omega\tau_v}}\right)\right]^{1/2}, \quad (9a,b)$$

where $\tau_v=2\rho_0 T/\Omega R_s$ and $\tau_e=N_{PR}\tau_v$.

The derivatives required for calculating surface wave group speed using the relaxation model are,

$$\frac{d\beta_W}{d\omega}=\frac{\mathrm{i}\Omega}{4\sqrt{T}}\left[\left(1+\frac{\gamma-1}{\sqrt{1-i\omega\tau_e}}\right)\left(1-\frac{1}{\sqrt{1-i\omega\tau_v}}\right)\right]^{-1/2}\left\{\frac{(\gamma-1)\tau_e}{(1-i\omega\tau_e)^{\frac{3}{2}}}\left(1-\frac{1}{\sqrt{1-i\omega\tau_v}}\right)-\frac{\tau_v\left(1+\frac{\gamma-1}{\sqrt{1-i\omega\tau_e}}\right)}{(1-i\omega\tau_v)^{\frac{3}{2}}}\right\}, \quad (10a)$$

$$\frac{dk_W}{d\omega}=\frac{\sqrt{T}}{c_0}\sqrt{\frac{1+\frac{\gamma-1}{\sqrt{1-i\omega\tau_e}}}{1-\frac{1}{\sqrt{1-i\omega\tau_v}}}}\left\{1+\frac{i\omega\tau_e(\gamma-1)}{4\left(1+\frac{\gamma-1}{\sqrt{1-i\omega\tau_e}}\right)(1-i\omega\tau_e)^{\frac{3}{2}}}+\frac{i\omega\tau_v}{4\left(1-\frac{1}{\sqrt{1-i\omega\tau_v}}\right)(1-i\omega\tau_v)^{\frac{3}{2}}}\right\}. \quad (10b)$$

The complex specific surface admittance and complex propagation constant of a surface with parallel slit-like pores of semi-width b, can be written in terms of complex compressibility, C_s, and complex Specific Volume, S_s (related to the inverse of complex density) as:

$$\beta_s=\frac{\Omega}{\sqrt{T}}(C_s S_s)^{\frac{1}{2}},\ k_s=\frac{\omega\sqrt{T}}{c_0}\left(C_s/S_s\right)^{\frac{1}{2}}, \quad (11a,b)$$

$$C_s=\frac{1}{\rho_0 c_0^2}\left[\gamma-(\gamma-1)\left(1-\tanh\left(\lambda\sqrt{-iN_{PR}}\right)/\lambda\sqrt{-iN_{PR}}\right)\right],\ S_s=\left[1-\tanh\left(\lambda\sqrt{-i}\right)/\lambda\sqrt{-i}\right] \quad (11c,d)$$

where $\lambda=b\sqrt{(\omega\rho_0/\mu)}$. The derivatives required for calculating the surface wave group speed using this model are:

$$\frac{d\beta_s}{d\omega}=\frac{1}{2}\beta_s\left(\frac{dC_s/d\omega}{C_s}+\frac{dS_s/d\omega}{S_s}\right),\ \frac{dk_s}{d\omega}=\frac{k_s}{\omega}+\frac{1}{2}k_s\left(\frac{dC_s/d\omega}{C_s}-\frac{dS_s/d\omega}{S_s}\right), \quad (11e,f)$$

$$\frac{dC_s}{d\omega}=\frac{\gamma-1}{2\omega\rho_0 c_0^2}\left[\left(1-\tanh^2\left(\lambda\sqrt{-iN_{PR}}\right)\right)-\frac{\tanh\left(\lambda\sqrt{-iN_{PR}}\right)}{\lambda\sqrt{-iN_{PR}}}\right],$$
$$\frac{dS_s}{d\omega}=\left[\frac{1}{2\omega}\right]\left[\frac{\tanh\left(\lambda\sqrt{-i}\right)}{\lambda\sqrt{-i}}-\left(1-\tanh^2\left(\lambda\sqrt{-i}\right)\right)\right] \quad (11g,h)$$

1.2. Comparative predictions of surface wave dispersion and attenuation

Figure 1 compares predictions of surface wave dispersion for a 0.04 m thick rigid-porous layer with Ω = 0.15, R_s = 5 kPa s m^{-2} and T = 2.5. These parameters correspond to a porous asphalt [6]. The relationship between the flow resistivity, tortuosity and porosity of a porous medium in which the pores are identical slits inclined at angle θ to the surface normal is $R_s=12\mu T/\Omega b^2$, where μ is

the dynamic viscosity of air, b is the slit semi-width and $T = 1/(\cos\theta)^2$. The values $\Omega = 0.15$, R_s = 5 kPa s m^{-2} and $T = 2.5$ correspond to slits of width 0.85 mm inclined at 50.7° to the surface normal.

The predictions according to the thin air layer approximation depart considerably from those of the other models for these porous layer parameters. Hamet, Wilson and slanted slit model predictions of surface wave phase speeds agree below 1 kHz. But above 1 kHz, Hamet and Wilson model predict that the surface wave phase speed increases with frequency. Hamet, Wilson and slanted slit model predictions of group speeds are similar, but all models predict that the surface wave group speed is lower than the phase speed at any given frequency.

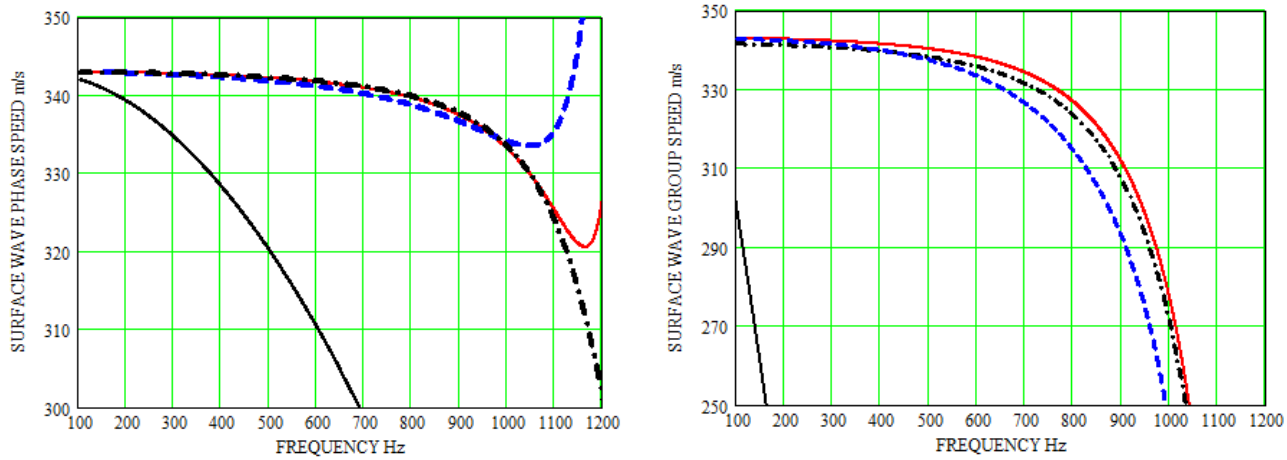

Figure 1: Predictions of surface wave speeds as a function of frequency over a hard backed 0.04 m thick, porous layer ($\Omega = 0.15$, R_s = 5 kPa s m^{-2} and $T = 2.5$): (a) phase speed (b) group speed: black dash-dot line slanted slits, black continuous line thin air layer approximation, red continuous line Wilson, blue broken line Hamet.

Figure 2 compares predictions of the horizontal and vertical attenuation constants for the surface wave. The predictions of the vertical attenuation constant agree closely. The differences in the predictions of the horizontal attenuation constant are not important since it is relatively small.

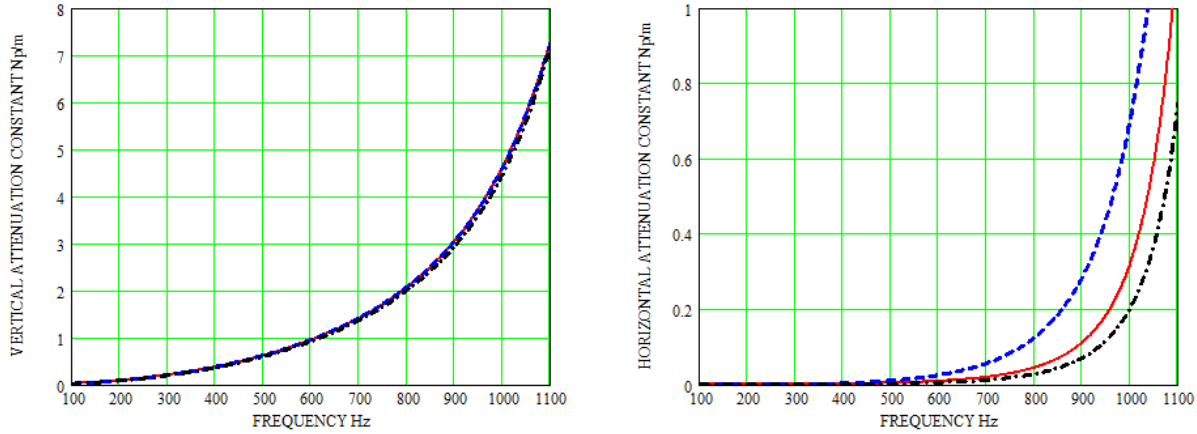

Figure 2: Predictions of vertical and horizontal attenuation constants for the surface wave over a hard backed 0.04 m thick, porous layer ($\Omega = 0.15$, R_s = 5 kPa s m^{-2} and $T = 2.5$): black dash-dot line slanted slits, red continuous line Wilson, blue broken line Hamet.

The predicted Excess Attenuation spectrum (see section 2.1) for point source and receiver at 0.04 m height separated by 2 m over 0.04 m thick rigid-porous layer with $\Omega = 0.15$, R_s = 5 kPa s m^{-2} and $T = 2.5$, allowing for extended reaction because of the low flow resistivity [1] and using the slit pore model, suggests the creation of a surface wave with main energy at 1100 Hz.

According to the predictions in Fig.1, at 1100 Hz, the surface wave group speed is 156 m/s i.e. 184 m/s less than the assumed speed of sound in air of 340 m/s. At a range of 2 m, this would

correspond to a time delay of 11 ms between the direct arrival of a 1 ms long direct pulse at 1100 Hz and the arrival of the surface wave pulse. According to the predictions in Fig. 2, at 1100 Hz the vertical attenuation of the surface wave is about 7.5 Nepers/m (65 dB/m). The corresponding horizontal attenuation is smaller, but it would be more than 7 dB/m in addition to that from cylindrical spreading.

2. COMPARISONS OF PREDICTIONS AND DATA OVER PARALLEL STRIPS

2.1. Excess attenuation spectra

Sound propagation from a point source over a locally reacting or impedance plane can be represented by spectra of the Excess Attenuation (EA) defined by

$$EA = 20\log\left(\frac{P_{total}}{P_{direct}}\right) \tag{12}$$

where P_{total} and P_{direct} are the total sound pressure levels with and without the impedance plane present respectively.

A comb-like surface can be formed by closely and regularly spaced parallel identical acoustically hard strips, normal to an acoustically hard surface. The gaps between them form parallel identical slit-like pores with tortuosity $\boldsymbol{T}$ = 1. Horizontal propagation through the strips is not possible, so such a layer is inherently locally reacting.

Figures 3(a) and 3(b) compare laboratory data for EA spectra over arrays of parallel identical regularly-spaced 0.0253 m high aluminium strips with predictions using (i) the analytical slit pore model (equations 12) and a numerical Boundary Element method (BEM) [5]. The edge-to-edge spacings were (a) 0.003 m and (b) 0.0124 m. The parameter values used for the hard-backed slit-pore layer predictions (broken red lines) are listed in Table 1 and based on the strip array geometries with T=1.

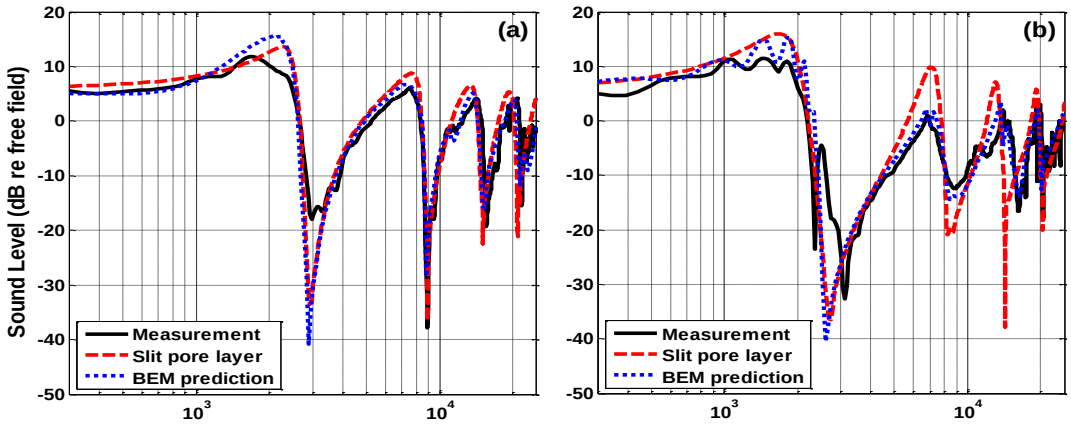

Figure 3: Measured excess attenuation spectra (black continuous lines) over parallel aluminium strips of height 0.0253 m placed on MDF board with uniform edge-to-edge spacing of (a) 0.0030 m (b) 0.0124 m compared with predictions using the slit pore layer model (broken red lines) and BEM (broken blue lines). Source and receiver are separated by 0.7 m and at 0.045 m height above the MDF board.

Table 1: Flow resistivity and porosity for 0.0253 m high aluminium strips with uniform edge-to-edge spacings. The coefficient of dynamic viscosity of air $\mu = 1.811 \times 10^{-5}$ m^2s^{-1}.

Edge-to-edge spacing 'a' (m)	Flow resistivity (Pa s m^{-2})	Porosity
0.003	125.6	0.1923
0.0124	2.85	0.496

If a surface wave is created during near-grazing propagation from a point source, it results in values in an EA spectrum that exceed +6 dB, which is the maximum pressure increase due to coherent reflection above a hard surface. Data and predictions in Figure 3 suggest that the main surface wave energy is near 1.8 kHz for both edge-to-edge separations.

The slit-pore layer predictions assume a hard backing, whereas the BEM predictions allow for the finite surface impedance of the MDF board. EA spectra obtained over the MDF board alone are fitted using a 2-parameter variable porosity model [1] with effective flow resistivity 10 MPa s m^{-2} and effective porosity rate 1.0 m^{-1}. The MDF board departs increasingly from an acoustically hard surface as frequency increases. So, increasing differences with increasing frequency between the slit pore layer and BEM predictions can be attributed, at least in part, to the finite MDF impedance.

2.2. Surface wave speed and attenuation estimates

Figure 4(a) shows (smoothed) time domain waveforms measured at three receiver heights (0.03 m, 0.07 m and 0.15 m) above the base of an array of parallel aluminium strips with edge-to-edge spacing of 0.0124 m. Figure 8(b) shows the corresponding measurements of EA spectra. The source used for these measurements was a Tannoy® driver attached to a 2 m long tube, the open end of which is assumed to act as a point source. The first peaks in the measured waveforms (Fig.4(a)) which commence before 8 ms and have magnitudes that increase with receiver height, so can be attributed to a combination of direct and coherent surface-reflected components whereas the approximately sinusoidal wave trains after ~8.5 ms, have magnitudes that decrease with height and may be attributed to surface waves.

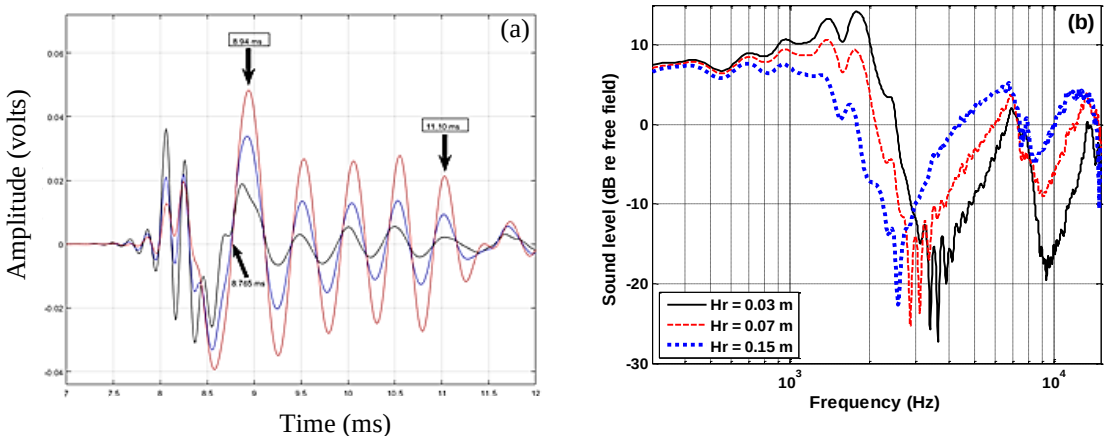

Figure 4: (a) smoothed measured time domain signals and (b) measured excess attenuation spectra over aluminium strips placed on MDF board with edge-to-edge spacing of 0.0124 m with receiver heights of 0.03 m (red trace), 0.07 m (blue trace) and 0.15 m (black trace), source at height of 0.045 m and source-receiver separation 0.7 m. Source and receiver heights are above the MDF base.

The first oscillation in the surface waveform for the lowest receiver height indicates that the surface wave period is 0.57 ms, thereby suggesting a main surface wave frequency of 1754 Hz, close to the frequencies of the corresponding maxima in the measured EA spectra. The first zero crossing of the surface waveform for the lowest receiver height is at 8.765 ms and that for the direct wave arrival is at 7.5 ms. The slowness formula

$$1/c_g = 1/c_0 + \Delta t/d \tag{13}$$

with c_0 = 343 m/s, $\Delta t = (8.765 - 7.5) \times 10^{-3}$ s and $d = 0.7$ m, can be used to estimate that the surface wave group speed is 211.7 m/s.

Figure 5(a) shows the surface wave dispersion measured using a phase gradient method over strips with edge-to-edge spacing of 0.0124 m compared with predictions using the admittance either that predicted by the slit pore model or the admittance deduced by fitting EA data [5]. The fitted

admittance leads to better agreement with data. The nominal slit depth of 0.0253 m gives rise to the prediction represented by the broken blue line in Fig. 5(a). A modal analysis of propagation over uniform grooves [8] suggests an effective depth of $d^{'} = d - a\log(2)/\pi$ where a is the edge-to-edge spacing. If a = 0.0124 m this gives an effective depth of 0.024 m.

Figure 5(b) shows the frequency-dependent surface wave phase (dash dot blue curve) and group (speeds predicted using this effective depth. At 1754 Hz the predicted phase speed is 309 m/s and the predicted group speed is 187 m/s. The predicted group speed is 12% lower than that estimated from the waveform for the lowest height in Fig. 4(a) (211.7 m/s).

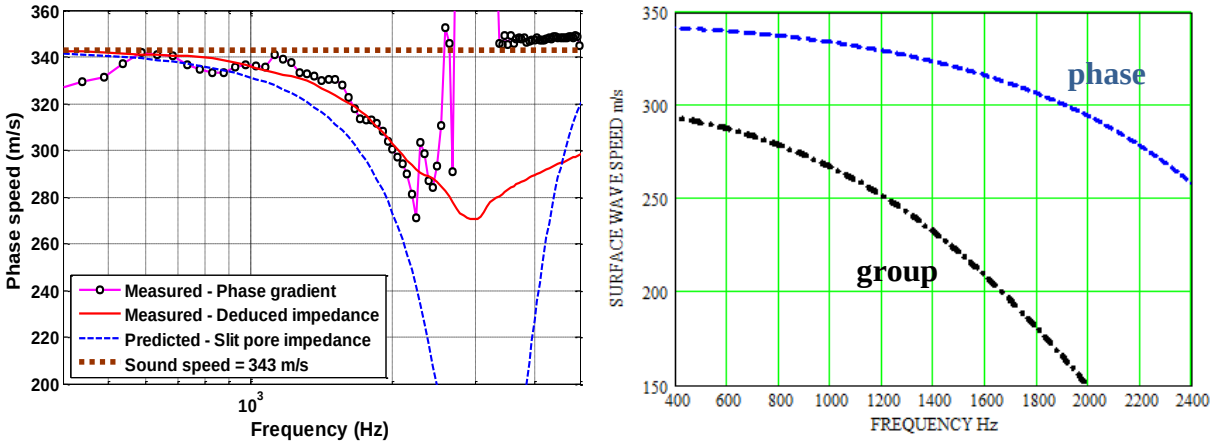

Figure 5: (a) Surface wave dispersion (joined circles) measured over aluminium rectangular strips with edge-to-edge spacing of 0.0124 m compared with predictions using the admittance deduced from complex excess attenuation data (solid red line) and that obtained by using the slit pore layer impedance model using the actual slit depth of 0.0253 m [5] (b) surface wave speeds predicted using the slit pore impedance model with an effective slit depth of 0.024 m: phase speed is given by the blue dash curve; the group speed by the black dash-dot curve.

Figure 7(a) shows a plot of the first surface waveform peak amplitudes measured over aluminium strips, with edge-to-edge spacing of 0.0124 m, as a function of receiver height. Also shown is an exponential curve with a fitted vertical attenuation of 15.96 nepers/m [5]. This is close to the value of 15.6 nepers/m predicted by the Hamet, Wilson and slit pore models at 1754 Hz assuming an effective slit depth of 0.024 m (Fig.7(b)).

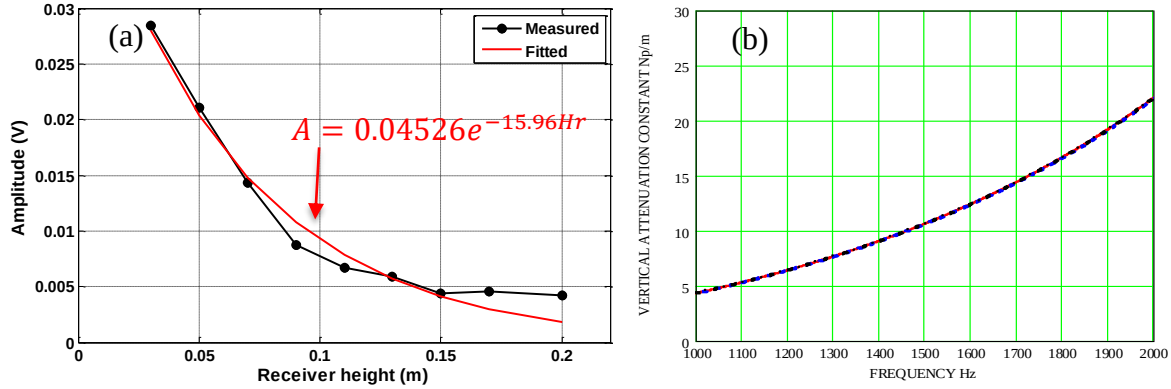

Figure 7(a): Measured amplitudes of the first peaks in the surface waveforms (joined black-circles) and fitted exponential curve (red continuous line) above 0.0253 m high aluminum strips placed on MDF board with edge-to-edge spacing of 0.0124 m at different receiver heights of 0.03 m, 0.04 m, 0.05 m, 0.06 m, 0.07 m, 0.08 m, 0.09 m and 0.10 m. The source at height is 0.03 m and the source-receiver separation is 0.7 m. Source and receiver heights are with respect to the MDF board base. Also shown is fitted exponential curve [5].

(b) predictions of the vertical attenuation constant of the surface wave as a function of frequency using Hamet, Wilson and slit pore models with an effective slit depth of 0.024 m.

3. CONCLUSIONS

Analytic expressions for the phase and group speeds and horizontal and vertical attenuation rates of airborne surface waves above hard-backed porous layers or parallel strips on a hard boundary have been derived from thin air layer, Hamet, Wilson and slit pore models. If parameters corresponding to a porous asphalt layer are used, both Hamet and Wilson models lead to unphysical predictions of surface wave dispersion above 1 kHz. Using the slit pore model, predicted surface wave characteristics are in close agreement with those deduced from measurements over arrays of parallel aluminum strips on MDF board.

4. ACKNOWLEDGEMENTS

We gratefully acknowledge the contributions to this paper of measurements made by Imran Bashir during research that received funding from the European Community's Seventh Framework Programme (FP7/2007-2013) under grant agreement n° 234306, collaborative project HOSANNA.

5. REFERENCES

1. Attenborough, K. and Van Renterghem, T. *Predicting Outdoor Sound* 2nd edition, Taylor and Francis, 2021.
2. Kelders, L. Lauriks, W. & Allard, J-F. Surface waves above thin porous layers saturated by air at ultrasonic frequencies. *J. Acoust. Soc. Am.,* **104**, 882 (1998).
3. Smith, F. C., Shin, H-C., & Attenborough K. Generation of Modally Pure Acoustic Surface Waves in a Tapered Partially-filled Duct, *Wave Motion* **40,** 29 – 40 (2004).
4. Donato, R. J. Model experiments on surface waves, *J. Acoust. Soc. Am.* **63**, 700 – 703 (1978).
5. Imran Bashir, *Acoustical exploitation of rough, mixed impedance and porous surfaces outdoors,* PhD Thesis, Open University (2014).
6. Berengier, M.C., Stinson, M.R., Daigle, G.A. & Hamet, J.-F., Porous road pavements: acoustical characterisation and propagation effects, J. Acoust. Soc. Am. 101 555 – 162 (1997).
7. Wilson, D. K., Simple relaxation models for the acoustical properties of porous media, *Applied Acoustics* **50** 171-188 (1997).
8. Kelders, L. Allard, J. F. & Lauriks, W. Ultrasonic surface waves above rectangular-groove gratings, *J. Acoust. Soc. Am.,* **103** 2730 (1998).